

Cooling Penetration into Normal and Injured Brain via Intraparenchymal Brain Cooling Probe: Theoretical Analyses

LIANG ZHU¹ and AXEL J. ROSENGART²

¹Department of Mechanical Engineering, University of Maryland Baltimore County, Baltimore, Maryland, USA

²Neurocritical Care and Acute Stroke Section, Departments of Neurology and Surgery (Neurosurgery), The University of Chicago Pritzker School of Medicine, Chicago, Illinois, USA

The selective cooling of severely injured brain tissue while maintaining normal temperature throughout the remaining body, to avoid cooling-related systemic side effects, has been proposed as a desirable method to improve the outcome of patients with acute brain catastrophes. One approach for targeted brain cooling may utilize miniature cooling probes directly inserted into injured brain tissue. Based on experimental data obtained in primates with normal and injured brains, this study simulates the expected temperature distributions surrounding a prototype brain cooling probe. Our model employs the Pennes bioheat equation to define the effects of local brain perfusion rate on the temperature field within brain tissue. Cooling penetration achieved by this probe under normal and globally ischemic conditions extended from 10 mm to 25 mm, respectively, from the device surface into the surrounding brain parenchyma, and was strongly dependent on the local brain perfusion, with a larger cooling penetration being obtained in injured (less perfused) brain regions. Further, the simulated results indicate that transient brain temperature behavior is affected by both the initial perfusion rate and the blood perfusion response to tissue cooling. Assuming a constant local blood perfusion rate during cooling, our model predicts an established steady state temperature field within 16 min, though additional time may be needed if the blood perfusion rate keeps changing during the cooling. It is also concluded that the brain cooling rate monitored by a temperature sensor close to the device may not be the most accurate measure of cooling penetration, as this estimate neglects to consider key variables such as local blood perfusion rate, monitoring location, and time duration over which the cooling rate is calculated.

INTRODUCTION

Brain hypothermia is an increasingly utilized treatment applied to improve outcome in many [1–3] but not all [4, 5] forms of severe brain injury. Brain cooling is initiated immediately in the acute phase of injury and is primarily directed at mitigating secondary neurologic injuries to vulnerable brain tissue. Animal models and experience with brain-injured humans suggest increasing beneficial effects of brain hypothermia with increasing cooling depth and duration; in addition, clinical studies have shown already that temperature reductions by 1 or 2°C below

37°C can improve outcome in patients with stroke, head injury, or after cardiac arrest. The main effects of brain hypothermia are reduction of tissue oxygen demands [6, 7] and amelioration of numerous deleterious cellular biochemical mechanisms, including calcium shift, excitotoxicity, lipid peroxidation and other free-radical reactions, DNA damage, and inflammation [8]. Hypothermia during experimental cerebral ischemia provides potent, dose-related, and long-lasting neuro-protection [9, 10]. Conversely, elevated brain temperature of only 1 to 2°C strikingly worsens experimental neuronal injury [11, 12] and clinical outcome [13].

Currently, brain hypothermia is achieved by applying whole body (systemic) cooling, which not only is cumbersome to initiate and control but also invariably leads to significant complications. Depending on the cooling depth and duration, the decrease in body temperature incurred during therapeutic hypothermia

Drs. Zhu and Rosengart are equally contributing lead authors.

Address correspondence to Dr. Liang Zhu, Department of Mechanical Engineering, University of Maryland Baltimore County, 1000 Hilltop Circle, Baltimore, MD 21250. E-mail: zliang@umbc.edu

will, over time, lead to cardiac arrhythmia, imbalances of fluid and electrolytes, lung and blood pressure failure, clotting abnormalities, and infections, thereby markedly limiting the clinical applications and the benefit-risk ratio of the practice [14]. In fact, many of the observed outcome inconsistencies among studies applying systemic hypothermia to patients with various brain injuries may be due to complications of systemic cooling confounding the neuroprotective benefit of brain hypothermia. For these reasons, selective or targeted brain cooling, which would achieve brain hypothermia without inducing significant body cooling, has been of intense research interest in recent years.

Experimental designs for targeted brain cooling range from somewhat simplistic approaches, such as cooling helmets [15, 16] and ice packing of the head or neck surface [17–19], to more invasive methods, such as nasopharyngeal cooling [20, 21] or direct brain tissue (intraparenchymal) cooling [22]. Head surface cooling via helmet or ice is practicable and easy to apply [16, 23–25], even in the pre-hospital settings; however, it does not penetrate beyond the upper brain surface [26–28]. While invasive brain cooling may seem inappropriately aggressive to be a useful neuroprotective therapy in humans, modern neurocritical care of severely brain-injured victims does presently advocate invasive, multi-modal brain monitoring and therapy, including brain instrumentation, such as placement of drainage catheters, electrodes, and other probes. For example, routine neurocritical care [12] includes the insertion of both rigid and flexible drainage catheters in order to drain ventricular fluid and to measure brain temperature and pressure. Such devices are placed at the bedside into the brain parenchyma through a small hole drilled in the skull, and, measuring between 3 and 5 mm in diameter, the catheters are subsequently advanced to the central parts of the brain without imaging guidance. For the treating neurocritical care clinicians, it is conceivable that modifications of such techniques could easily incorporate direct brain-cooling devices, such as a combined brain fluid drainage and cooling catheter. The complications and side effects are similar to that induced by the drainage catheters.

The successful development of the practice of selective brain cooling should be based on a thorough understanding of the heat transfer within normally and abnormally perfused brain tissue, specifically, the time required to reach a steady-state temperature field after initiation of focal brain cooling. Furthermore, the temperature distribution and cooling penetration emitted from a focal cooling source within the parenchyma under various physiological and pathological conditions must be considered, as well as the relation of such findings to the actual cooling capacity and physical proportions of the cooling device. In patients at high risk for brain injury (e.g., intraoperative patients during brain surgery) or in already brain-injured victims, *hypoperfusion* of brain parenchyma (i.e., due to expanding mass lesions such as blood clots or edema) is commonly present [29]. It is expected that the cooling zone would cover a larger tissue region for these patients.

In this study, we used a primate model to investigate a novel intraparenchymal cooling device and study its performance de-

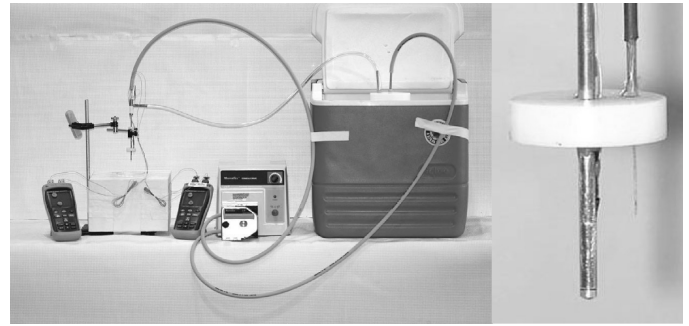


Figure 1 The cooling system and the brain-cooling probe.

pendent on the regional blood perfusion under both healthy and physiological conditions, and during brain perfusion (circulatory) arrest. The governing rationale was to gain an understanding about the temperature fields and transient cooling behavior of a first-of-its-kind intra-parenchymal brain cooling device. The obtained results would provide valuable information for future device design modifications and an approximation for its potential clinical applicability. For example, the developed theoretical model could be utilized in future clinical settings to optimize the overlap between expected and targeted brain cooling regions and to define a priori the most favorable treatment decisions. Neuroscientists and researchers at the University of Chicago and Argonne National Laboratory developed this cooling system (U.S. patent pending) currently employed in animal studies. It consists of a cooling shaft, a slurry ice bath, a variable-speed circulation pump, and two digital recorders for temperature acquisition, as shown in Figure 1. Figure 2 provides a more detailed schematic drawing of the probe. The cooling device itself consists of a dual-lumen, and a one-inch long stainless steel shaft with an outer diameter of 2.7 mm, a wall of 0.17 mm, and an inner diameter of 2.4 mm. A cooling solution pump distributes coolant first into the inner tube, then out the distal end of the shaft through an outlet, finally

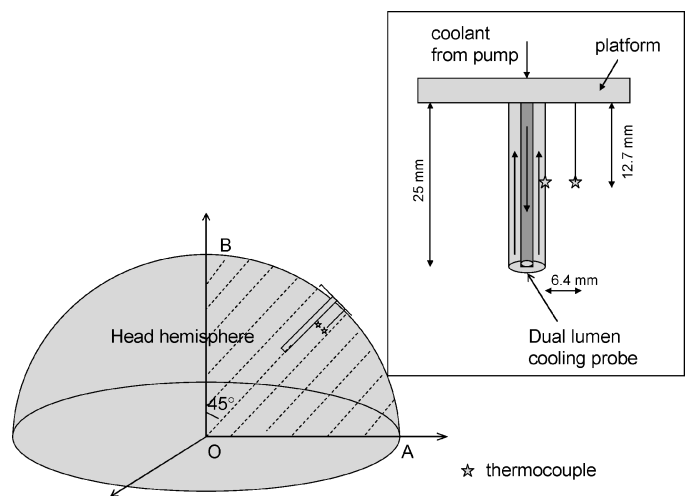


Figure 2 Schematic diagram of the structure of the cooling probe and its inserted location inside the brain tissue. Note that two temperature sensors are implemented in the device.

returning the coolant via the larger, outer tube back to the cooling reservoir.

In all experiments, the probe was inserted in the radial direction directly into the brain. One thermocouple was positioned at the outer wall of the cooling shaft, and the other was located 6.4 mm from the probe surface to provide real-time temperature measurements during the experiments. The thermocouples (copper-constantan, 0.25 mm in diameter, OMEGA, Stamford, Connecticut, USA) and cooling probe were mounted onto a platform to maintain the predetermined spatial relationship throughout the brain cooling experiments (see Figures 1 and 2). Thermocouple readings were recorded and stored electronically.

In this study, the Pennes bioheat equation [30] was selected to model the blood perfusion effect in brain tissue. We simulated the temperature field within the brain tissue to estimate the cooling depth surrounding the probe and the cooling propagation after probe insertion into the perfused brain. Our model was validated by comparing the theoretically predicted temperature transients to the measured data obtained in the animal experiments. We further investigated the temperature fields in the human brain as affected by both local blood perfusion and by the blood perfusion response to the cooling.

MATHEMATICAL MODELING

The Pennes bioheat equation was selected as the basis for mathematical modeling. This equation views blood perfusion throughout the brain as a heat source/sink, a value that is assumed to be proportional to the local blood perfusion rate and the difference between the arterial blood and local tissue temperature [15, 28]. This widely known continuum model by Pennes [30] is shown in Eq. (1). Originally applied to predict temperature fields in the human forearm, this equation is a modification of the ordinary heat conduction equation with two extra heat source/sink terms:

$$\rho c \frac{\partial T_i}{\partial t} = k_t \nabla^2 T_i + (\rho c)_{blood} \omega (T_a - T_i) + q_m \quad (1)$$

where k_t is the thermal conductivity of tissue, ρ is the tissue density, c is the specific heat of tissue, ω is the local blood perfusion rate, and q_m is the local metabolic heat generation rate. T_i is tissue temperature and T_a arterial blood temperature.

The previously developed theoretical model [15] of temperature distribution in the human head has been modified for the current application. The brain is modeled as a hemisphere with several layers. The first layer represents the scalp, and the second layer represents the skull. Because both brain gray and white matters may have different blood perfusion rates, they are represented by different layers as shown in Figure 3

Assuming homogeneous thermal properties within each layer, we write the three-dimensional Pennes bioheat equations

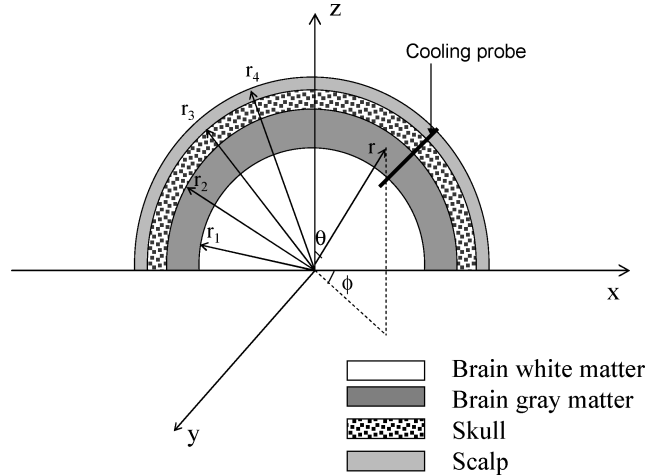


Figure 3 Simplified brain cooling model includes several layers of head structure. The cooling probe is not drawn in this figure and is treated as a boundary condition of known temperature in the simulation. r represents the radius of each spherical structure: $r_1 = 67$ mm, $r_2 = 85$ mm, $r_3 = 89$ mm, and $r_4 = 93$ mm.

in spherical coordinates for each layer as:

$$\left\{ \begin{array}{l} \text{for scalp:} \\ (\rho c)_{sc} \frac{\partial T_{sc}}{\partial t} = \frac{k_{sc}}{r^2} \left[\frac{\partial}{\partial r} \left(r^2 \frac{\partial T_{sc}}{\partial r} \right) + \frac{1}{\sin \theta} \frac{\partial}{\partial \theta} \left(\sin \theta \frac{\partial T_{sc}}{\partial \theta} \right) \right. \\ \left. + \frac{1}{\sin^2 \theta} \frac{\partial^2 T_{sc}}{\partial \phi^2} \right] + (\rho c)_{blood} \omega_{sc} (T_a - T_{sc}) + q_{m,sc} \\ \text{for bone:} \\ (\rho c)_{bone} \frac{\partial T_{bone}}{\partial t} = \frac{k_{bone}}{r^2} \left[\frac{\partial}{\partial r} \left(r^2 \frac{\partial T_{bone}}{\partial r} \right) \right. \\ \left. + \frac{1}{\sin \theta} \frac{\partial}{\partial \theta} \left(\sin \theta \frac{\partial T_{bone}}{\partial \theta} \right) + \frac{1}{\sin^2 \theta} \frac{\partial^2 T_{bone}}{\partial \phi^2} \right] \\ \left. + (\rho c)_{blood} \omega_{bone} (T_a - T_{bone}) + q_{m,bone} \right. \\ \text{for brain gray matter:} \\ (\rho c)_{bt,g} \frac{\partial T_{bt,g}}{\partial t} = \frac{k_{bt,g}}{r^2} \left[\frac{\partial}{\partial r} \left(r^2 \frac{\partial T_{bt,g}}{\partial r} \right) \right. \\ \left. + \frac{1}{\sin \theta} \frac{\partial}{\partial \theta} \left(\sin \theta \frac{\partial T_{bt,g}}{\partial \theta} \right) + \frac{1}{\sin^2 \theta} \frac{\partial^2 T_{bt,g}}{\partial \phi^2} \right] \\ \left. + (\rho c)_{blood} \omega_{bt,g} (T_a - T_{bt,g}) + q_{m,bt,g} \right. \\ \text{for brain white matter:} \\ (\rho c)_{bt,w} \frac{\partial T_{bt,w}}{\partial t} = \frac{k_{bt,w}}{r^2} \left[\frac{\partial}{\partial r} \left(r^2 \frac{\partial T_{bt,w}}{\partial r} \right) \right. \\ \left. + \frac{1}{\sin \theta} \frac{\partial}{\partial \theta} \left(\sin \theta \frac{\partial T_{bt,w}}{\partial \theta} \right) + \frac{1}{\sin^2 \theta} \frac{\partial^2 T_{bt,w}}{\partial \phi^2} \right] \\ \left. + (\rho c)_{blood} \omega_{bt,w} (T_a - T_{bt,w}) + q_{m,bt,w} \right. \end{array} \right. \quad (2)$$

where subscript sc , $bone$, bt,g , and bt,w represent scalp, bone, brain tissue gray matter, and brain tissue white matter, respectively. At the interfaces between different layers, the temperature and heat flux continuities are satisfied. On the bottom of the hemisphere, an adiabatic condition is assumed. Since the head

is exposed to room temperature ($T_{air} = 20^\circ\text{C}$), the boundary condition on the scalp surface is subject to a surface convection of $h = 8 \text{ W/m}^2 - \text{K}$, which is determined from a heat transfer textbook [31].

Cooling probe insertion into the brain surface is $\theta = 45^\circ$ at a polar angle, penetration of the cooling tip is 25 mm from the scalp surface, and ϕ is the zenithal angle, as shown in Figure 2. For simplicity, in the model, the cooling probe is represented as a straight line of 25 mm in length inside the brain tissue, as illustrated in Figure 3. The cooling probe is shown as a boundary condition along this line of 6°C , which was documented during a primate experiment. The initial condition of the transient heat transfer equation, $T_0(r, \theta, \phi)$, is equal to the established steady-state temperature field in the brain before the probe is inserted. The boundary and initial conditions are given by:

$$\begin{aligned}
 r = 0 : \frac{\partial T_{bt,w}}{\partial r} &= 0 \\
 r = r_1 : T_{bt,g} = T_{bt,w}, \quad k_{bt,g} \frac{\partial T_{bt,g}}{\partial r} &= k_{bt,w} \frac{\partial T_{bt,w}}{\partial r} \\
 r = r_2 : T_{bone} = T_{bt,g}, \quad k_{bone} \frac{\partial T_{bone}}{\partial r} &= k_{bt,g} \frac{\partial T_{bt,g}}{\partial r} \\
 r = r_3 : T_{sc} = T_{bone}, \quad k_{sc} \frac{\partial T_{sc}}{\partial r} &= k_{bone} \frac{\partial T_{bone}}{\partial r} \\
 r = r_4 : -k_{sc} \frac{\partial T_{sc}}{\partial r} &= h(T_{sc} - T_{air}) \quad (3) \\
 \theta = 45^\circ, \text{ and } r_4 - 0.025 < r < r_4 : T_{bt,w,bt,g,bone,sc} &= 6^\circ\text{C} \\
 \theta = \frac{\pi}{2}, 0 : \frac{\partial T_{sc,bone,bt,g,bt,w}}{\partial \theta} &= 0, T_{sc,bone,bt,g,bt,w}(r, \theta, \phi) \\
 &= T_{sc,bone,bt,g,bt,w}(r, \theta, \phi + 2\pi) \\
 t = 0 : T_{sc,bone,bt,g,bt,w} &= T_0(r, \theta, \phi)
 \end{aligned}$$

The explicit scheme of the finite difference method is chosen as the numerical method to solve for the partial differential equation in this formulation. The time and spatial derivatives are approximated by forward and central differences, respectively. Two factors, computational accuracy and time required to solve the equation system, are considered in the selection of the number and placement of the nodes in the discretization. The more nodes there are, the more accurate the solution will be; however, with each additional node, more time will be needed to solve the 3-D equation system. A finer nodal network near the cooling device is necessary to ensure adequate computing accuracy of heat conduction near the device, while a coarser network far away from the device is more computationally efficient in significantly reducing the computing time of the simulation process and the required storage space of the simulation results.

In this study, the grid size in the radial direction Δr is uniform and equal to 1 mm. In the other two angular directions, we implement non-uniform grid sizes. In the region surrounding the cooling device ($30^\circ < \theta < 60^\circ$ and $0^\circ < \phi < 30^\circ$), grid size is $\Delta\theta = \Delta\phi = 1.875^\circ$, while the grid sizes are $\Delta\theta = \Delta\phi = 7.5^\circ$ in the rest of the simulated region. The explicit scheme is used in this study for simplicity; however, the explicit implementation of the finite difference method is only conditionally stable. In this study, the stability condition of the explicit method applied is satisfied by reducing the time step below a certain limit. The upper limit is determined and the actual time step is selected as 0.00001 second, which would not cause oscillation during the numerical simulation. The discretized equation for node (i, j, k) is given by:

$$\begin{aligned}
 \frac{T_{i,j,k}^{n+1} - T_{i,j,k}^n}{\Delta t} &= \frac{k}{\rho c} \left[\frac{T_{i+1,j,k}^n - T_{i,j,k}^n}{\Delta r_{i+1}} - \frac{T_{i,j,k}^n - T_{i-1,j,k}^n}{\Delta r_i} \right] \\
 &\times \left(\frac{2}{\Delta r_{i+1} + \Delta r_i} \right) + \frac{k}{\rho c} \frac{2}{r_i} \frac{T_{i+1,j,k}^n - T_{i-1,j,k}^n}{\Delta r_i} \\
 &+ \frac{k}{\rho c} \frac{1}{r_i^2} \left[\frac{T_{i,j+1,k}^n - T_{i,j,k}^n}{\Delta\theta_{j+1}} - \frac{T_{i,j,k}^n - T_{i,j-1,k}^n}{\Delta\theta_j} \right] \\
 &\times \left(\frac{2}{\Delta\theta_{j+1} + \Delta\theta_j} \right) + \frac{k}{\rho c} \frac{ctg\theta_j}{r_i^2} \frac{T_{i,j+1,k}^n - T_{i,j-1,k}^n}{(\Delta\theta_j + \Delta\theta_{j+1})/2} \\
 &+ \frac{k}{\rho c} \frac{1}{r_i^2} \frac{1}{\sin^2\theta_j} \left[\frac{T_{i,j,k+1}^n - T_{i,j,k}^n}{\Delta\phi_{k+1}} - \frac{T_{i,j,k}^n - T_{i,j,k-1}^n}{\Delta\phi_k} \right] \\
 &\times \left(\frac{2}{\Delta\phi_{k+1} + \Delta\phi_k} \right) + \frac{(\rho c)_{blood}\omega(T_a - T_{i,j,k}^n)}{\rho c} + \frac{q_m}{\rho c} \quad (4)
 \end{aligned}$$

where T^{n+1} and T^n represent temperatures of the node associated with the new and previous times, respectively. The temperature continuity at any interface is satisfied, as the node is selected at the interface of the two adjacent regions. The heat flux continuity is discretized as the rate equation for the node at the interface.

Based on the algorithm, a FORTRAN code has been written and runs on a personal computer. The program has been tested to ensure that the variations in the grid size or time step would yield less than 0.1% of the maximal temperature variation in the simulated domain.

RESULTS

Model Validation

To validate this model, theoretical predictions were compared with two sets of measurements captured in primate brain experiments [22]. The protocol of the animal experiment has been reviewed and approved by the IACUC at the University of

Table 1 Physical and physiological properties under normal conditions for the monkey brain

	Specific heat c (J/kg.K)	Density ρ (kg/m ³)	Thermal conductivity k (W/m.K)	Perfusion rate ω_0 (ml/min·100 g tissue)	Metabolism q_m (W/m ³)	Radius r (mm)
Scalp	4000 [†]	1000 [‡]	0.34 [‡]	2.0	363.4*	60
Skull	2300*	1500 [‡]	1.16 [‡]	1.8	368.4*	58
Brain tissue	3700*	1050 [‡]	0.5 [‡]	35–80	7306–16700*	56

*Xu et al. [36].

[†]Dexter and Hinderman [38].[‡]Olsen et al. [39].

Nelson and Nunneley [26].

^{||}Kito et al. [32], Noda et al. [33].

Chicago. Two female macaca fascicularis monkeys between 1.5 and 2 years old and weighting 1.8 kg to 2.8 kg were used. Each monkey underwent general anesthesia using isoflurane after ketamine induction. Room temperature was maintained at 20°C. The animals were covered to maintain a normal rectal temperature. Blood pressure and heart rate were maintained in each animal at baseline values throughout the *in vivo* experiments. Partial unilateral parieto-temporal craniectomy with splitting of the dura was performed, followed by insertion of the cooling probe into the brain parenchyma. Special care was taken to use only a single, minimally traumatic device insertion and to position the cooling shaft and satellite thermocouple so as to be completely surrounded by brain parenchyma (i.e., avoiding areas close to ventricles). After insertion, the cooling device was firmly affixed to the animal's head frame, and the surgical wound was covered with gauze. The coolant was then pumped into the cooling device, and the temperatures at all measuring locations were electronically recorded and stored. After the experiment, the animal was euthanized with an intra-cardiac potassium chloride injection.

Based on the brain geometric measurements obtained after the experiment, the monkey brain was modeled as a hemisphere of 56 mm in radius. As the blood perfusion rate was not measured during the animal study, in this model, the blood perfusion effects of the brain white and gray matters were considered to be the same. The blood perfusion rate used in this model may be considered an average value of both the white and gray matters. Table 1 gives all the physical and physiological properties of the primate under normal conditions. Note that the metabolic rate under normal conditions is coupled with the average blood perfusion rate, and both are unchanged during the cooling.

The surface temperature of the probe did not change significantly after it was inserted into the brain tissue and was maintained around 6°C. Transient temperatures measured by the satellite intra-parenchymal thermocouple are represented by the scattered symbols in Figure 4. The theoretical prediction of the temperature transient at the same location is also plotted in Figure 4, where the thicker line represents the situation when the blood perfusion rate is selected as 35 ml/(min·100 g tissue), and the thinner line represents the situation when $\omega = 80$ ml/(min·100 g tissue). The characteristic times to reach steady state for the experimental study were around 500 seconds and

250 seconds, respectively. Although the blood perfusion rate was not measured directly during the animal experiments, comparing the theoretical predictions to the experimental data suggests that the theoretical predictions strongly agree with the animal data when the blood perfusion rate is chosen from the range between 35 and 80 ml/(min·100 g tissue). The normal range of blood perfusion rates used here is supported by current literature [32, 33], in which the values in the monkey vary from 30 to 100 ml/(min·100 g tissue).

Parametric Study

Table 2 gives all the physical and physiological properties under normal conditions used in the human brain model. A preponderance of the current literature shows that the blood perfusion rate of gray matter varies from 50 to 85 ml/(min·100 g tissue). Blood perfusion rate in white matter is about one-fourth that of gray matter and varies from 15 to 27 ml/(min·100 g tissue). In this study, the blood perfusion rates in the gray and white matters are selected as 80 and 20 ml/(min·100 g tissue), respectively, as shown in Table 2. The volumes of gray and white

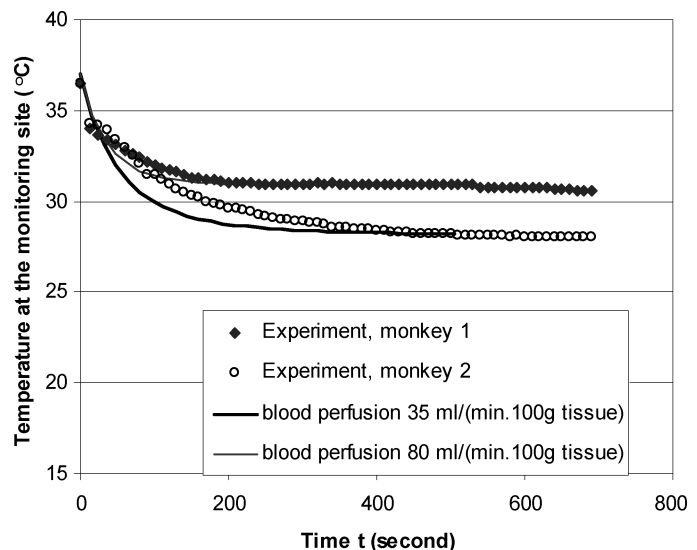
**Figure 4** Comparison between experimentally measured and theoretical prediction of temperatures at the monitoring site.

Table 2 Physical and physiological properties under normal conditions for the human brain

	Specific heat c (J/kg.K)	Density ρ (kg/m ³)	Thermal conductivity k (W/m.K)	Perfusion rate ω_0 (ml/min·100g tissue)	Metabolism q_m (W/m ³)	Radius r (mm)
Scalp	4000*	1000 [‡]	0.34 [‡]	2.0	363.4*	93
Skull	2300*	1500 [‡]	1.16 [‡]	1.8*	368.4*	89
Gray matter	3700*	1050 [‡]	0.5 [‡]	80*	16700*	85
White matter	3700*	1050 [‡]	0.5 [‡]	20*	4175*	67
Blood	3800 [†]	1050 [‡]	0.5 [‡]	—	—	—

*Xu et al. [36].

[†]Dexter and Hinderman [38].

[‡]Olsen et al. [39].

[§]Nelson and Nunneley [26].

matters are selected so that the volumetric-average blood perfusion rate of the brain tissue is approximately 50 ml/(min·100 g tissue). Although the simulation provides a three-dimensional temperature field in the brain tissue, the following figures are presented only to illustrate the temperature distribution on the shadowed area (plane AOBA) containing the cooling probe, as shown in Figure 2.

The steady-state temperature distribution in the vicinity of the cooling probe is shown in Figure 5, in which temperature contours are plotted. In this study, cooling is considered significant if the steady-state temperature is less than 36°C, which is illustrated by the thicker solid contour line in Figure 5. Due to the length limitation of the probe, only an approximately 10 mm layer of the white matter is cooled. Most of the cooling occurs in the gray matter. Cooling penetration is apparently limited to the vicinity of the cooling probe, 10 mm along the axial direction of the probe and 19 mm laterally from the probe surface.

In the parametric study, we evaluate the effect of local blood perfusion rate on the cooling penetration and the time required to reach a steady state temperature field. Figure 6 demonstrates

how variation of the blood perfusion rate of the white matter may affect the cooling region ($T_{bt,g}$ and $T_{bt,w} < 36^\circ\text{C}$). All the parameters are the same as they appear in Table 2 except that $\omega_{bt,w}$ is selected as 15, 20, and 30 ml/(min·100 g), respectively. Notice that $\omega_{bt,w}$ has some effect on the temperature field in the white matter region. However, this effect is insignificant, as it produces a less than 5% change in the penetration depth of the cooling probe.

The variation of the temperature contour of 36°C, shown in Figure 7, illustrates the important role played by the blood perfusion rate of the gray matter. The lower limit of the blood perfusion rate under normal conditions is 50 ml/(min·100 g tissue), as represented by the solid line in Figure 7. During brain ischemia, blood perfusion rate in brain can be significantly reduced from its normal value. In this study, the resulting temperature field in the ischemic brain tissue ($\omega_{bt,g} = 16$ ml/(min·100 g tissue)) is represented by the double dashed line in Figure 7. The significant decrease in $\omega_{bt,g}$ from 80 ml/(min·100 g tissue) to 50 ml/(min·100 g tissue) and to 16 ml/(min·100 g tissue) results in an overall increase in the cooling penetration. This trend is more evident in the situation of brain ischemia. The lateral cooling penetration depth can be as much as 25 mm from the device surface.

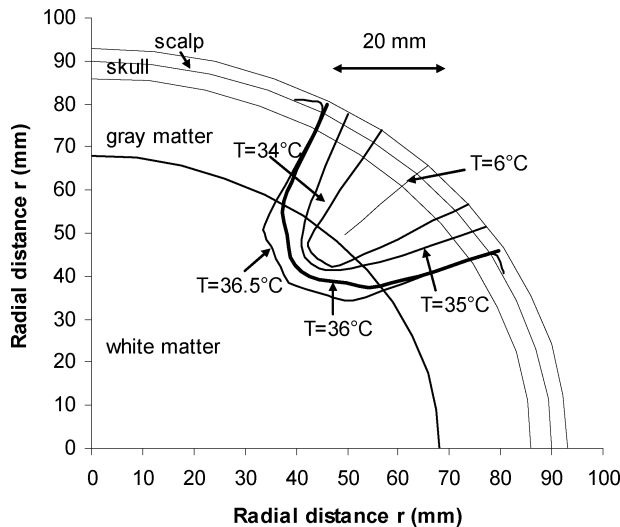


Figure 5 Isotherms of the steady-state temperature distribution in the vicinity of the cooling probe under normal conditions. Cooling penetration depths are similar in both lateral and axial directions in tissue.

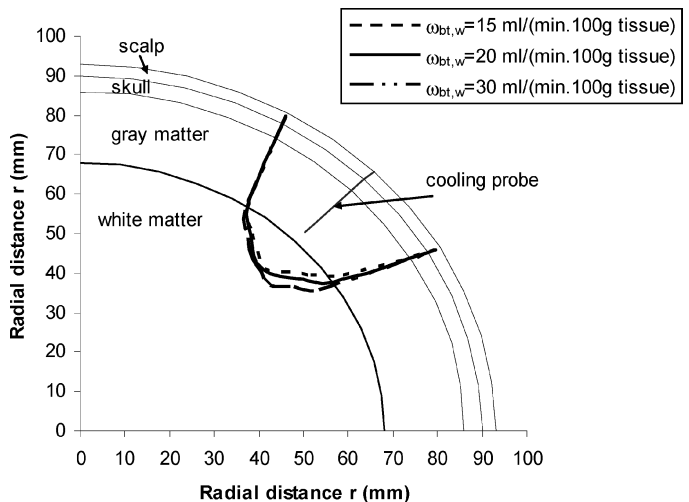


Figure 6 Effect of the local blood perfusion rate in the white matter on the cooling penetration. Temperature contour represents the isotherm of 36°C.

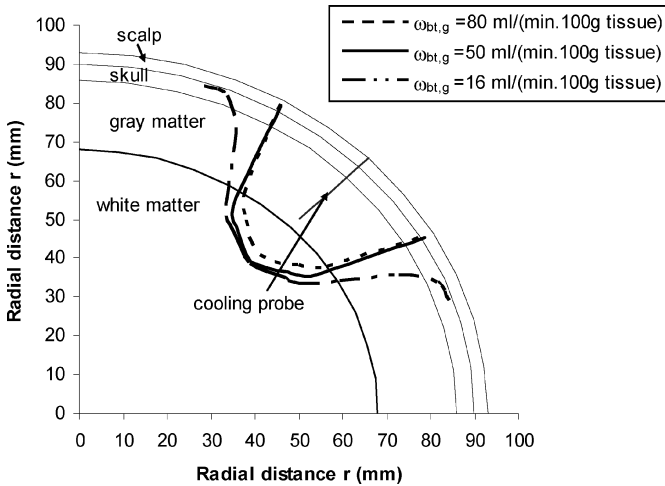


Figure 7 Deeper cooling penetration induced by decreasing the blood perfusion rate in the gray matter (from 80 to 16 ml/min·100 g tissue). Temperature contour represents isotherm of 36°C.

Similar to our previous paper [15], the time required to establish a steady state is defined as

$$\frac{T(r, \theta, \phi, t_c) - T(r, \theta, \phi, 0)}{T_c(r, \theta, \phi) - T(r, \theta, \phi, 0)} = 99\% \quad (5)$$

where $T(r, \theta, \phi, 0)$ is the initial temperature before the cooling and $T_c(r, \theta, \phi)$ is the steady-state temperature after the cooling. Table 3 gives the time it takes to reach the steady state. In general, it takes more time to reach the steady-state temperature distribution in the brain tissue when the blood perfusion rate is smaller. Under normal conditions, as listed in Table 2, the time required to reach the steady state is around 11 minutes; however, more than 16 minutes may be needed to reach the equilibration for patients with brain ischemia.

Both the local blood perfusion rate and metabolism in the brain tissue may change due to the temperature reduction induced by the cooling process. Earlier experimental studies [34, 35] have shown a linear relationship between $1/T$, where T is tissue temperature, and $\log CMRO_2$ (the cerebral metabolic rate of oxygen consumption). A mathematical expression of this relationship can then be given as

$$CMRO_2 = CMRO_{2,n} \cdot Q_{10}^{\frac{T-37}{10}} \quad (6)$$

where $CMRO_{2,n}$ is the normal cerebral metabolic rate of oxygen consumption, and Q_{10} is called Q_{10} value, which has been reported between 2 and 4.4 [35]. This law states that the metabolic

rate decreases by a factor of Q_{10} with each 10°C reduction in temperature. Based on a Q_{10} value of 3, it has been calculated that hypothermia decreases the cerebral metabolic rate by an average value of 9% for the first 1°C reduction in temperature, while the metabolic rate is reduced to one-third of the normal value when the temperature reduction is 10°C. In this study, we select the Q_{10} value as 3 and assume that the metabolic heat generation, q_m , in the brain tissue follows the expression,

$$q_m = q_{m0} 3^{(T_{bt}-T_a)/10} \quad (7)$$

where T_a is the arterial temperature of 37°C, T_{bt} is the local brain tissue temperature, and q_{m0} is the metabolic heat generation rate under normal conditions, as listed in Table 2. During normal conditions, local blood perfusion rate is coupled with local metabolic heat generation [36]. The temperature-dependent ω_{bt} in the brain tissue could then be proposed as:

$$\omega_{bt} = \omega_{bt,0} 3^{(T_{bt}-T_a)/10} \quad (8)$$

where $\omega_{bt,0}$ is the blood perfusion rate under normal conditions (37°C). Figure 8 depicts the propagation of the temperature contour of 36°C into the deep brain tissue at different time instances, when ω_{bt} is temperature-dependent. The reduced blood perfusion rates in both white and gray matters lead to a deeper cooling penetration in tissue, which further results in a lower blood perfusion rate. If the temperature-dependent relationship continues during the cooling, it may take a much longer time to reach steady state.

A distant thermocouple with a fixed spatial relationship to the cooling device was employed in the brain tissue; it was located at a distance of 6.4 mm perpendicular to the length of the probe shaft, reaching 12 mm into brain parenchyma (Figure 2). In the prototype cooling device, the cooling rates (°C/second) measured at the location were used to evaluate the level of local blood perfusion. The effect of local blood perfusion rate on the temperature transient of this location is illustrated in Figure 9. The change in $\omega_{bt,w}$ can be seen to have a very minor effect on the temperature transient recorded by the thermocouple. Alternately, the effect of $\omega_{bt,g}$ is evident, as the initial cooling rate recorded at this site becomes sensitive to the local blood perfusion rate in the gray matter. While typically (within a fixed time period prior to the steady state) a more rapid cooling rate is associated with a lower local blood perfusion rate, if the cooling rate is calculated within a long time duration, this cooling rate may actually become increasingly insensitive to the blood perfusion rate, as a lower blood perfusion rate results in a lower

Table 3 Characteristic time to reach steady-state temperature distribution in the brain

Effect of the blood perfusion in the white matter $\omega_{bt,w}$ (ml/min·100 g tissue)			Effect of the blood perfusion in the gray matter $\omega_{bt,g}$ (ml/min·100 g tissue)		
$\omega_{bt,w} = 15$	$\omega_{bt,w} = 20^*$	$\omega_{bt,w} = 30$	$\omega_{bt,g} = 16$	$\omega_{bt,g} = 50$	$\omega_{bt,g} = 80^*$
672 (s)	640 (s)	480 (s)	976 (s)	736 (s)	640 (s)

*normal conditions as listed in Table 2.

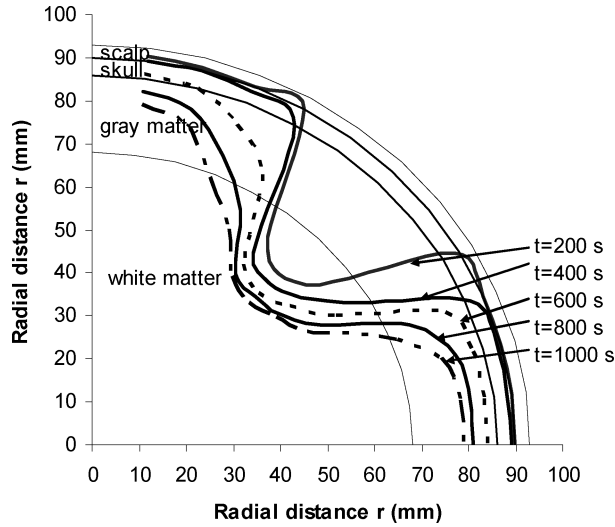


Figure 8 Propagation of the isotherm (36°C) during the cooling processes when the blood perfusion is coupled with the temperature-dependent metabolic heat generation.

steady-state temperature. Again, however, the time required to reach this steady state is longer.

DISCUSSION

There are several limitations associated with this theoretical modeling. The actual geometry of the human head is not a hemisphere, as assumed here. Additionally, each layer inside the head has been simplified to correspond to this hemisphere representation. However, as illustrated by the modeling, the temperature variation induced by the cooling probe is confined within a small vicinity of the probe (up to 25 mm). Temperature is almost uniform in the rest of the brain tissue. Therefore, the inaccuracy of the brain geometry may not have a significant effect on the induced temperature field.

The other limitation of the theoretical model involves any boundaries inherent in the Pennes bioheat equation used in the simulation. It is still not clear how accurate the Pennes bio-

heat equation is in modeling the blood flow effect in the brain tissue. Further, as with most continuum models in which the heat and mass transport are averaged over a representative control volume, the Pennes bioheat equation is unable to simulate point-to-point temperature variation in the vicinity of any large discrete blood vessel. However, as shown in van Leeuwen et al. [27], the predicted temperature contours based on detailed, discrete vasculature in the brain are consistent with that predicted by the Pennes equation. Therefore, the Pennes equation can still provide a reasonable prediction of the brain temperature field. The agreement of the current model with the temperature measurement at one tissue site in the animal study further suggests a reasonable accuracy of the theoretical study. Inclusions of additional details of the brain geometry and vasculature into the theoretical model would further optimize the predictive value of the computations.

Future experiments should utilize modified intraparenchymal cooling devices with multiple, strategically-located temperature sensors throughout the surrounding brain parenchyma to allow a higher temperature field resolution. Further, model validation would be enhanced with measured rather than estimated blood perfusion rates during cooling. However, real-time brain perfusion measurements represent a significant experimental and operative challenge, especially if it is desired to delineate transient perfusion. Similar to many other investigators, we utilized the original validation of the Pennes bioheat equation [30] and adjusted the blood perfusion rate to obtain the best fit to the experimental data. In support of this approach is the fact that the fitted perfusion values were within the range known to be physiologic for macaca fascicularis monkeys, the subspecies used in our studies. Furthermore, reviewing the current clinical and animal literature on brain hypothermia, none of the previous studies using the more commonly known techniques (e.g., microsphere, MRI, laser Doppler flowmeter) measured continuously blood perfusion rates during targeted brain cooling, likely because of limitations in technical feasibility. An exception to this is a previous paper of one of the authors [37], in which the blood flow rate of the common carotid artery (in the neck) of rats was continuously measured during head surface cooling. Although we selected rats of similar weight and size, the blood flow response was quite different from one rat to another. The variability of the blood flow response makes the theoretical simulation complicated. We wish to develop a similar technique in the future to address the limitation of the current experiment.

Confirming the conclusions drawn in previous theoretical studies [15, 28], our model, based on data from primate experiments, identifies the sensitivity of the simulated temperature field to be the absolute value of the local blood perfusion rate. As expected from the Pennes bioheat equation, local blood perfusion and brain metabolism act as heat sources during selective brain cooling. The strength of this heat source is typically proportional to the temperature difference between the arterial blood and tissue and the local blood perfusion rate. Thus, under normal conditions, brain temperature does not deviate much from the average arterial temperature of approximately 37°C [26, 28]. In

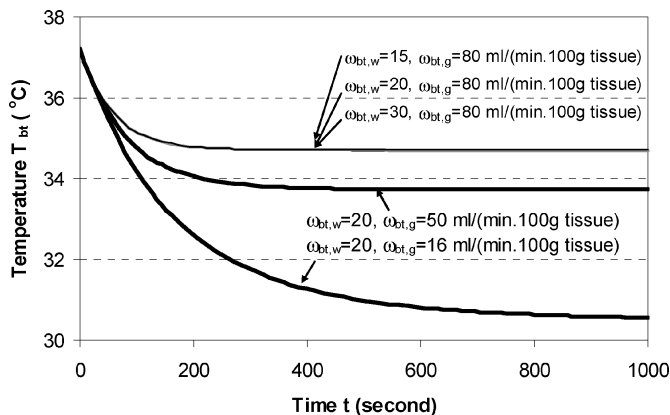


Figure 9 Effect of the blood perfusion rate of either the gray or white matter on the temperature transient at the monitoring site.

the case of using an intra-parenchymal (tissue) cooling probe, as in our experiments, increases in the local perfusion rate and/or blood temperatures will lead to smaller cooling zones around the cooling device, because the cooled blood is more rapidly redistributed and diluted throughout the entire blood circulation. In contrast, in clinical settings where brain perfusion is either not present at all (e.g., ischemic core within a brain infarction) or markedly reduced (e.g., penumbra region around an ischemic brain core), both the blood perfusion rate and temperature less dominantly counteract the cooling effects of the probe, thus allowing the cooling zone to extend further laterally from the device when compared to cooling of non-injured brain. This finding has important clinical consequences with respect to the future development of targeted brain cooling devices. Severely ischemic brain regions allow extended cooling penetration throughout the brain, resulting in more efficient and easily obtainable temperature reductions and brain tissue protection. Over time, and with increasing blood perfusion and recovery of brain tissue, the maximum cooling front reduces accordingly. This inverse relationship between the achieved cooling area and the improving blood perfusion rate in brain ischemia during the acute phase of brain injury provides theoretical support for the use of focal, intraparenchymal cooling devices in brain injury.

As suggested by the theoretical modeling, the blood perfusion response to the local cooling may play an important role in determining the effectiveness of the cooling probe. In a recent study in rats [37], the transient blood flow rate in the carotid artery was monitored and measured during the head surface cooling. It was shown that, although the blood flow rate decreases with the temperature reduction in tissue, the characteristic time of the blood flow response can vary from 5 minutes to as long as 40 minutes. This is certainly a challenge in theoretical modeling in which the blood perfusion rate is not only a function of local temperature, but also a function of time and other factors. The current theoretical analysis, in which the blood perfusion is fixed during the cooling, can be viewed as an upper limit of the possible cooling penetration using this cooling probe.

Monitoring temperature directly in the brain is clinically important in assessing the actual cooling extent and its fluctuations with changes in systemic body temperature. To be useful for monitoring brain temperature during cooling therapy, temperature sensors must be placed in the vicinity of the cooling probe. The current theoretical modeling of the expected temperature gradients within the brain tissue will help to determine the optimal temperature monitoring site(s). It is important to note here that the relationship between a measured steady-state cooling temperature within the brain parenchyma and the actual cooling rate at the monitoring site can be used to interpret changes in local blood perfusion rate, and hence provide an indirect marker of worsening brain ischemia and injury.

In summary, our theoretical simulation based on cooling experiments in the primate model has provided a temperature field in the vicinity of an intra-parenchymal cooling probe. For our prototype cooling device inserted directly into the brain tissue, the cooling penetration varied between 10 mm and 25 mm from

the probe surface and depended strongly on the local blood perfusion rate. Brain ischemia promotes the cooling penetration, resulting in a larger cooling region for injured brain tissue. The simulated results have also shown that the transient behavior is affected by both the local blood perfusion rate and the blood perfusion response to the local cooling. The cooling rate alone may not be an accurate measure of the extent of cooling, as it strongly depends on the monitoring location, blood perfusion rate, and time duration. The current theoretical evaluation further increases our understanding of temperature distributions in both normally and abnormally perfused brain tissue regions during intra-parenchymal brain cooling. Our results can be applied to assist with the development of clinically useful cooling devices for targeted brain hypothermia.

ACKNOWLEDGMENTS

The authors are grateful to R. Loch McDonald, M.D., Ph.D., at the University of Chicago for the opportunity to use a primate animal model for the experimental evaluation of our cooling probe. The authors also gratefully appreciate the support of Kenneth E. Kasza, Ph.D., and Jeffrey E. Franklin and their team at Argonne National Laboratory, Argonne, Illinois, for substantial support in the design of the intra-parenchymal cooling probe and obtaining the animal data. Furthermore, the authors thankfully acknowledge the veterinarians and support staff at the Carlson Animal Research Facility at the University of Chicago.

This research was supported by the Brain Research Foundation at the University of Chicago, the Cancer Research Foundation, Chicago (A.J.R.), and the American Heart Association (grant 0160320U to L.Z.).

NOMENCLATURE

c	specific heat capacity, J/kgK
h	heat transfer coefficient, W/m ² K
k	thermal conductivity, W/mK
Q_{10}	Q_{10} value
q_m	local metabolic heat generation rate, W/m ³
r	radial distance in spherical coordinate, m
r_1	radius of the layer of brain white matter, m
r_2	radius of interface between brain gray matter and skull, m
r_3	radius of interface between skull and scalp, m
r_4	radius of head, m
t	time, s
T	temperature, °C or K

Greek Symbols

ϕ	zenithal angle in spherical coordinate, rad
θ	polar angle in spherical coordinate, rad

ρ	density, kg/m ³
ω	local blood perfusion rate, 1/s or ml/min·100 g tissue

Subscripts

0	normal conditions
<i>a</i>	artery
<i>bt</i>	brain tissue
<i>bt, g</i>	brain tissue, gray matter
<i>bt, w</i>	brain tissue, white matter
<i>m</i>	metabolism
<i>sc</i>	scalp
<i>t</i>	tissue

REFERENCES

- [1] Bernard, S. A., Gray, T. W., Buist, M. D., Jones, B. M., Silvester, W., Gutteridge, G., and Smith, K., Treatment of Comatose Survivors of Out-of-Hospital Cardiac Arrest with Induced Hypothermia, *New England Journal of Medicine*, vol. 346, no. 8, pp. 557–563, 2002.
- [2] McIntyre, L. A., Fergusson, D. A., Hebert, P. C., Moher, D., and Hutchison, J. S., Prolonged Therapeutic Hypothermia after Traumatic Brain Injury in Adults: A Systematic Review, *JAMA*, vol. 289, pp. 2992–2999, 2003.
- [3] Nolan, J. P., Morley, P. T., Vanden Hoek, T. L., and Hickey, R. W., Advanced Life Support Task Force of the International Liaison Committee on Resuscitation Therapeutic Hypothermia after Cardiac Arrest. An Advisory Statement by the Advanced Life Support Task Force of the International Liaison Committee on Resuscitation, *Circulation*, vol. 108, pp. 118–121, 2003.
- [4] Alderson, P., Gadkary, C., and Signorini, D., Therapeutic Hypothermia for Head Injury, *Cochrane Database Syst. Rev.*, vol. 18, no. 4, CD001048, 2004. Available online at <http://mrw.interscience.wiley.com/cochrane/clsystrev/articles/CD0010408/frame.html>
- [5] Clifton, G. L., Miller, E. R., Choi, S. C., Levin, H. S., McCauley, S., Smith, K. R. Jr., Muizelaar, J. P., Wagner, F. C. Jr., Marion, D. W., Luerssen, T. G., Chesnut, R. M., and Schwartz, M., Lack of Effect of Induction of Hypothermia after Acute Brain Injury, *New England Journal of Medicine*, vol. 344, no. 8, pp. 556–563, 2001.
- [6] Illievich, U. M., Zornow, M. H., Choi, K. T., Scheller, M. S., and Srnat, M. A., Effects of Hypothermic Metabolic Suppression on Hippocampal Glutamate Concentrations after Transient Global Cerebral Ischemia, *Anesth. Analg.*, vol. 78, pp. 905–911, 1994.
- [7] Rosomoff, H. L., and Holaday, D. A., Cerebral Blood Flow and Cerebral Oxygen Consumption during Hypothermia, *American Journal of Physiology*, vol. 179, pp. 85–88, 1954.
- [8] Polderman, K. H., Application of Therapeutic Hypothermia in the ICU: Opportunities and Pitfalls of a Promising Treatment Modality, Part 1: Indications and Evidence, *Intensive Care Medicine*, vol. 30, no. 4, pp. 556–575, 2004.
- [9] Busto, R., Dietrich, W. D., Globus, M. Y., Valdes, I., Scheinberg P., and Ginsberg, M. S., Small Differences in Intra Ischemic Brain Temperature Critically Determine the Extent of Ischemic Neuronal Injury, *Journal of Cerebral Blood Flow Metabolism*, vol. 7, pp. 729–738, 1987.
- [10] Nurse, S., and Corbett, D., Direct Measurement of Brain Temperature during and after Intraischemic Hypothermia: Correlation with Behavioral, Physiological, and Histological Endpoints, *Journal of Neuroscience*, vol. 14, pp. 7726–7734, 1994.
- [11] Minamisawa, H., Smith, M. L., and Siesjö, B. K., The Effect of Mild Hyperthermia and Hypothermia on Brain Damage Following 5, 10, and 15 Minutes of Forebrain Ischemia, *Ann. Neurol.*, vol. 28, pp. 26–33, 1990.
- [12] Wijdicks, E. F. M., *The Clinical Practice of Critical Care Neurology*, pp. 129–147, Oxford University Press, Inc., New York, 2003.
- [13] Jiang, J. Y., Gao, G. Y., Li, W. P., Yu, M. K., and Zhu, C., Early Indicators of Prognosis in 846 Cases of Severe Traumatic Brain Injury, *Journal of Neurotrauma*, vol. 19, no. 7, pp. 869–874, 2002.
- [14] Polderman, K. H., Application of Therapeutic Hypothermia in the Intensive Care Unit. Opportunities and Pitfalls of a Promising Treatment Modality, Part 2: Practical Aspects and Side Effects, *Intensive Care Medicine*, vol. 30, no. 5, pp. 757–769, 2004.
- [15] Diao, C., Zhu, L., and Wang, H., Cooling and Rewarming for Brain Ischemia or Injury: Theoretical Analysis, *Annals of Biomedical Engineering*, vol. 31, pp. 346–352, 2003.
- [16] Wang, H., Olivero, W., Lanzino, G., Elkins, W., Rose, J., Honings, D., Rodde, M., Burnham, J., and Wang, D., Rapid and Selective Cerebral Hypothermia Achieved Using a Cooling Helmet, *Journal of Neurosurgery*, vol. 100, pp. 272–277, 2004.
- [17] Bommadevara, M., and Zhu, L., Temperature Difference between the Body Core and Arterial Blood Supplied to the Brain During Hyperthermia or Hypothermia in Humans, *Biomechanics & Modeling in Mechanobiology*, vol. 1, no. 2, pp. 137–149, 2002.
- [18] Furuse, M., Ohta, T., Ikenaga, T., Liang, Y. M., Isono, N., Kuroiwa T., and Preul, M. C., Effects of Intravascular Perfusion of Cooled Crystalloid Solution on Cold-Induced Brain Injury Using an Extracorporeal Cooling-Filtration System, *Acta Neurochir (Wien)*, vol. 145, no. 11, pp. 983–992, 2003.
- [19] Zhu, L., Theoretical Evaluation of Contributions of Heat Conduction and Countercurrent Heat Exchange in Selective Brain Cooling in Humans, *Annals of Biomedical Engineering*, vol. 28, no. 3, pp. 269–277, 2000.
- [20] Einer-Jensen, N., Baptiste, K. E., Madsen, F., and Khoroshii, M. H., Can Intubation Harm the Brain in Critical Care Situations? A New Simple Technique May Provide a Method for Controlling Brain Temperature, *Medical Hypotheses*, vol. 58, no. 3, pp. 229–231, 2002.
- [21] Hagioka, S., Takeda, Y., Takata, K., and Morita, K., Nasopharyngeal Cooling Selectively and Rapidly Decreases Brain Temperature and Attenuates Neuronal Damage, Even If Initiated at the Onset of Cardiopulmonary Resuscitation in Rats, *Critical Care Medicine*, vol. 31, no. 10, pp. 2502–2508, 2003.
- [22] Rosengart, A. J., Kasza, K., Zhu, L., Panchal, A., Macdonald, R. L., Chien, T., Franklin, J., Johns, L. M., Pytel, P., Novakovic, R., Wardrip, C., Frank, J. I., and Poeppel, R., Selective Brain Cooling: Understanding Brain Thermoconductivity Using a Primate Model, *American Academy of Neurological Surgeons 2004 (ANNS'04)*.
- [23] Battin, M. R., Penrice, J., Gunn, T. R., and Gunn, A. J., Treatment of Term Infants with Head Cooling and Mild Systemic Hypothermia (35.0°C and 34.5°C) after Perinatal Asphyxia, *Pediatrics*, vol. 111, pp. 244–251, 2003.
- [24] Iwata, O., Iwata, S., Tamura, M., Nakamura, T., Sugiura, M., Ogiso, Y., and Takashima, S., Early Head Cooling in Newborn Piglets is Neuroprotective Even in the Absence of Profound

- System Hypothermia, *Pediatrics International*, vol. 45, pp. 522–529, 2003.
- [25] Thoresen, M., Simmonds, M., Satas, S., Tooley, J., and Silver, I. A., Effective Selective Head Cooling during Posthypoxic Hypothermia in Newborn Piglets, *Pediatric Research*, vol. 49, no. 4, pp. 594–599, 2001.
- [26] Nelson, D. A., and Nunneley, S. A., Brain Temperature and Limits on Transcranial Cooling in Humans: Quantitative Modeling Results, *European Journal of Applied Physiology & Occupational Physiology*, vol. 78, no. 4, pp. 353–359, 1998.
- [27] van Leeuwen, G. M., Hand, J. W., Lagendijk, J. J., Azzopardi, D. V., and Edwards, A. D., Numerical Modeling of Temperature Distributions within the Neonatal Head, *Pediatric Research*, vol. 48, no. 3, pp. 351–356, 2000.
- [28] Zhu, L., and Diao, C., Theoretical Simulation of Temperature Distribution in the Brain during Mild Hypothermia Treatment for Brain Injury, *Med. & Bio. Eng. & Comput.*, vol. 39, pp. 681–687, 2001.
- [29] Ryan, M., Combs, G., and Penix, L. P., Preventing Stroke in Patients with Transient Ischemic Attacks, *American Family Physician*, vol. 60, pp. 2329–2341, 1999.
- [30] Pennes, H. H., Analysis of Tissue and Arterial Blood Temperatures in the Resting Human Forearm, *Journal of Applied Physiology*, vol. 1, pp. 93–122, 1948.
- [31] Incropera, F. P., and DeWitt, D. P., *Fundamentals of Heat and Mass Transfer*, 5th ed., John Wiley & Sons, Inc., Hoboken, NJ, 2002.
- [32] Kito, G., Nishimura, A., Susumu, T., Nagata, R., Kuge, Y., Yokota, C., and Minematsu, K., Experimental Thromboembolic Stroke in Cynomolgus Monkey, *Journal of Neuroscience Methods*, vol. 105, no. 1, pp. 45–53, 2001.
- [33] Noda, A., Ohba, H., Kakiuchi, T., Futatsubashi, M., Tsukada, H., and Nishimura, S., Age-Related Changes in Cerebral Blood Flow and Glucose Metabolism in Conscious Rhesus Monkeys, *Brain Research*, vol. 936, pp. 76–81, 2002.
- [34] Bering, E., Effect of Body Temperature Change on Cerebral Oxygen Consumption of the Intact Monkey, *American Journal of Physiology*, vol. 200, pp. 417–419, 1961.
- [35] Hoffman, W., Miletich, D. J., and Albrecht, R., Differential Cerebral Hypothermia, *Cryobiology*, vol. 19, pp. 392–401, 1982.
- [36] Xu, X., Tikuisis, P., and Giesbrecht, G., A Mathematical Model for Human Brain Cooling during Cold-Water Near-Drowning, *Journal of Applied Physiology*, vol. 86, no. 1, pp. 265–272, 1999.
- [37] Diao, C., and Zhu, L., Temperature Distribution and Blood Perfusion Response in Rat Brain during Selective Brain Cooling, *Medical Physics*, vol. 33, no. 7, pp. 2565–2573, 2006.
- [38] Dexter, F., and Hinderman, B. J., Computer Simulation of Brain Cooling during Cardiopulmonary Bypass, *Ann. Thorac. Surg.*, vol. 57, pp. 1171–1179, 1994.
- [39] Olsen, R. W., Hayes, L. J., Wissler, E. H., Nikaidoh, H., and Eberhart, R. C., Influence of Hypothermia and Circulatory Arrest on Cerebral Temperature Distributions, *ASME Journal of Biomechanical Engineering*, vol. 107, pp. 354–360, 1985.



Liang Zhu is an associate professor in the Department of Mechanical Engineering at the University of Maryland Baltimore County. She received her B.S. from the University of Science and Technology of China, Hefei, China, in 1988, and Ph.D. from the City University of New York, New York, in 1995. Her research is focused on fundamental heat transfer mechanisms in biological systems and temperature distribution in tissue during hypothermia or hyperthermia treatments.



Axel J. Rosengart is an assistant professor of neurology and neurosurgery and assistant director of the Neuroscience Critical Care and Acute Stroke Program at the University of Chicago. He received his M.D. from Christian Albrecht University, Kiel, Germany, in 1987, followed by clinical training and Ph.D. dissertation in Neuroscience at the University of Luebeck, Luebeck, Germany, in 1995. Among his current research interests are the development of novel bedside brain monitoring and cooling techniques in severely brain-injured patients as well as the design of functionalized nano-carriers for drug delivery and toxin removal.

Copyright of Heat Transfer Engineering is the property of Taylor & Francis Ltd and its content may not be copied or emailed to multiple sites or posted to a listserv without the copyright holder's express written permission. However, users may print, download, or email articles for individual use.